Novel epitaxy between oxides and semiconductors
– Growth and Interfacial Structures

Professor Minghwei HONG

Department of Materials Science and Engineering, National Tsing Hua University

Section 2, Kuang-Fu Rd., Hsinchu, Taiwan, Republic of China

Phone: 886-3-574-2283; FAX: 886-3-572-2366; mhong@mx.nthu.edu.tw

Technical milestones

1. ***epitaxial single crystal growth of γ-Al_2O_3 and other oxides on Si (111)***
2. ***growth of GaN on nano thick γ-Al_2O_3 and other single crystal oxides, which are epitaxially grown on Si (111)***
3. ***growth of GaN on c-plane sapphire Al_2O_3 using MOCVD and/or MBE***
4. ***high-resolution x-ray diffraction on (a) γ-Al_2O_3 and other oxides on Si (111); (b) hetero-structures of GaN/nano-thick γ-Al_2O_3 (and other oxides)/Si (111); and (c) GaN on c-plane sapphire Al_2O_3***

We have accomplished the above listed technical milestones and the technical results are summarized in this first-year (a three-year renewable grant) report. The report is organized in the following: Section I discusses growth and structural characteristics (including high-resolution x-ray diffraction and high-resolution transmission electron microscopy (HR-TEM)) of single crystal cubic γ-Al_2O_3 (different from the more common α-Al_2O_3 (sapphire) and cubic Sc_2O_3 on Si (111). This has included what was proposed to be studied in technical milestones 1 and 4 (a). Section II discusses molecular beam epitaxial (MBE) growth of GaN on nano thick γ-Al_2O_3 and Sc_2O_3 single crystal oxides, epitaxially grown on Si (111). This then includes what was proposed to be studied in technical milestone 2. Studies using in-situ reflection high energy electron diffraction (RHEED), high- resolution x-ray diffraction and HR-TEM performed on hetero-structures of GaN/nano thick γ-Al_2O_3 (Sc_2O_3)/Si (111) are discussed in Section II, which is the technical milestone 4(b). The results from technical milestones 3 and 4(c) will be discussed in Section III. A conclusion is given in Section IV in summarizing our first-year project. ***Section V lists the technical milestones to be accomplished in the second year.***

Report Documentation Page

Form Approved
OMB No. 0704-0188

1. REPORT DATE	2. REPORT TYPE	3. DATES COVERED
16 MAY 2007	**FInal**	**21-12-2005 to 16-05-2007**

4. TITLE AND SUBTITLE
Novel Epitaxy Between Oxides and Semiconductors ? Growth and Interfacial Structures

5a. CONTRACT NUMBER
FA520906P0093

5b. GRANT NUMBER

5c. PROGRAM ELEMENT NUMBER

6. AUTHOR(S)
Minghwei Hong

5d. PROJECT NUMBER

5e. TASK NUMBER

5f. WORK UNIT NUMBER

7. PERFORMING ORGANIZATION NAME(S) AND ADDRESS(ES)
National Tsing Hua University,101, Section 2, Kuang Fu Rd,Hsinchu 30055,Taiwan,TW,30055

8. PERFORMING ORGANIZATION REPORT NUMBER
N/A

9. SPONSORING/MONITORING AGENCY NAME(S) AND ADDRESS(ES)
AOARD, UNIT 45002, APO, AP, 96337-5002

10. SPONSOR/MONITOR'S ACRONYM(S)
AOARD

11. SPONSOR/MONITOR'S REPORT NUMBER(S)
AOARD-054094

12. DISTRIBUTION/AVAILABILITY STATEMENT
Approved for public release; distribution unlimited

13. SUPPLEMENTARY NOTES

14. ABSTRACT

The cubic gamma-Al2O3 and Si have significantly different atomic structures and lattice constants. The lattice constant of γ-Al2O3 is 7.91? and that of Si is 5.42 ?. Matching the two lattices over a unit cell dimension will result in a greater than 30% lattice mismatch. It is intriguing that a highly ordered epitaxial growth was obtained in an unusually large mismatch for a hetero-epitaxial system. High-quality single-crystal Sc2O3 films a few nanometer thick have been grown epitaxially on Si (111) despite a huge lattice mismatch. The films have the cubic bixbyite phase with a remarkably uniform thickness and high structural perfection. The bulk lattice constants of Si (5.43 ?) and Sc2O3 (9.86 ?) are mismatched by 9.2 % (relative to the doubled Si unit cell dimension). It is intriguing that a highly ordered epitaxial growth was obtained with this unusually large mismatch. It is demonstrated that epitaxial GaN layers are grown on substrates of c-plane sapphire or Si (111) wafers with gamma-Al2O3 or Sc2O3 buffer layers. Even though the of line widths of GaN grown on c-plane sapphire is smaller, the crystalline quality of the GaN grown on Si(111) with buffer layers are observed to be impressively good.

15. SUBJECT TERMS
Nanotechnology, Gallium Nitride

16. SECURITY CLASSIFICATION OF:			17. LIMITATION OF ABSTRACT	18. NUMBER OF PAGES	19a. NAME OF RESPONSIBLE PERSON
a. REPORT	b. ABSTRACT	c. THIS PAGE			
unclassified	**unclassified**	**unclassified**	**Same as Report (SAR)**	**32**	

I. Epitaxial single crystal growth of γ-Al_2O_3 and Sc_2O_3 on Si (111) and their structural properties

(a) *γ-Al_2O_3*

Brief summary

In this Section, we report the attainment of very high-quality cubic γ-Al_2O_3 single crystal films with thickness as thin as 3.8 nm. The oxide films have (111) as the normal in parallel with (111) of Si substrate and the films have [4 $\bar{4}$0] in-plane axis in parallel with [2 $\bar{2}$0] of the Si substrate. The rocking scans at γ-Al_2O_3 (222) position of films 3.8 and 11 nm shows a low full width at half maximum (FWHM) of 0.6 and 0.3 degree, respectively. Atomic force microscopy (AFM) and x-ray reflectivity (XRR) all show a very smooth surface about 0.1~0.2 nm. The oxide/Si interface is also atomically smooth of 0.1~0.2 nm as studied using XRR and cross-sectional HR-TEM.

I(a)-1 Introduction and Background

Hetero-epitaxial growth between insulators and semiconductors is always fascinating in science and important in technology.[1-5] For example, growth of single crystal GaN on sapphire[1] has been essential for producing blue lasers and LED's. Epitaxial growth of insulators on Si is another example, on which a subsequent single-crystalline growth of other semiconductors such as GaN[5] may integrate high-power microwave devices or lasers with the most advanced Si-based electronic devices.

Single crystal γ-Al_2O_3 films were reported to grow on Si (111) with mixed-sources molecular beam epitaxy (Al-N_2O MBE)[5-7]. To obtain higher-quality Al_2O_3 films, an Al layer ~ 1nm thick was pre-deposited at room temperatures on very thin SiO_x chemically formed on Si surface[5,6]. Then the substrate temperature was elevated to 800^0C to form an alumina template by the reaction between the pre-deposited Al and SiO_x. A γ-Al_2O_3 layer of 4 nm thickness was then grown using the MBE on the template at 800^0C. The claim on obtaining the γ-Al_2O_3 films was solely based on the observation and analysis of the reflection high energy electron diffraction (RHEED) patterns of Al_2O_3 and Si. The crystallographic

information on the thin Al_2O_3 films using x-ray diffraction and/or transmission electron diffraction has not been given.

In contrast to the previous efforts[5-7] using molecular beam epitaxy (MBE) with precursors or gases, a high-purity sapphire was employed in this work. E-beam evaporation was used due to the high melting point of sapphire, and the deposited species (incoming flux) consist of only Al_2O_3 molecules or clusters.

I(a)-2 Experimental

Si wafers 2-inch in diameter with (111) as the normal to the wafer plane were put into a multi-chamber MBE/UHV system[8], after being cleaned with an RCA method and an HF dip. Heating the Si wafers to temperatures above ~550^0C has resulted in a sharp, streaky 7x7 RHEED pattern with Kikuchi arcs (as shown in Fig. I-1 (a)), indicative of the attainment of a clean surface of Si (111) substrate. The wafers were then transferred under UHV (hence any possibility of Si oxidation was minimized and/or eliminated) to an oxide chamber for the Al_2O_3 deposition. During the oxide deposition, the vacuum in the chamber was maintained in the low 10^{-9} torr (even with the evaporation of sapphire) and substrate temperatures were maintained at about 700~750^0C. Streaky oxide RHEED patterns along the in-plane axes of [1 $\bar{1}$0] and [11 $\bar{2}$] (shown in figure 1b) of Si were observed after growth of oxide 1nm thick, indicating that a smooth single crystal γ-Al_2O_3 film formed on the Si (111) and with in-plane alignment between the oxide film and Si substrate.

Single crystal x-ray measurements were carried out on a four-circle triple-axes diffractometer, using a 12 kW rotating anode Cu K-alpha source. A pair of graphite crystals is used to monochromatize and analyze the x-ray beam with a resolution of 0.01 $Å^{-1}$ along the longitudinal and 0.005 $Å^{-1}$ along the transverse directions respectively. We have intentionally chosen this low resolution in order to increase the sensitivity to very thin films. The TEM sample analytical work is performed using a Philips TECNAI-20 FEG type TEM.

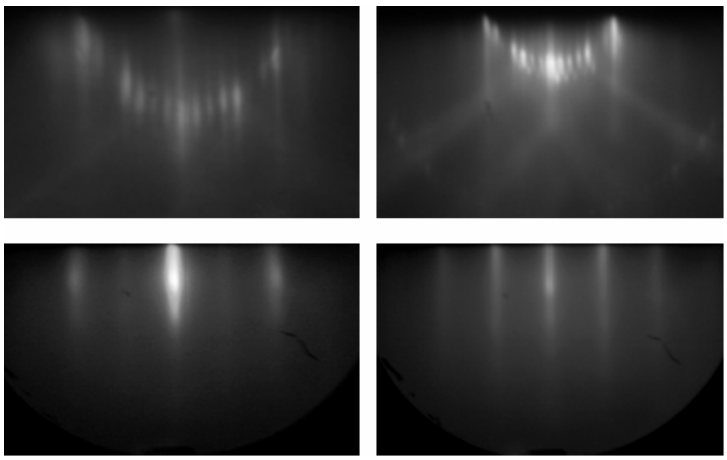

Fig. I-1 In-situ RHEED patterns of Si (111) substrate (a) and of γ-Al_2O_3 (111) film 1.0 nm thick (b) along [1 $\bar{1}$0] and [11 $\bar{2}$] axes. Note that the surface normal (111) γ-Al_2O_3 film is parallel with (111) Si and the in-plane axe [4 $\bar{4}$0] of γ-Al_2O_3 is in parallel with [2 $\bar{2}$0] of Si substrate.

I (a)-3 Results and Discussion

A single crystal x-ray theta two-theta scan along substrate surface of Si (111) on the oxide film 3.8 nm thick is shown in Figure I-2, in which a broad peak near 40 degree coincides with the (222) reflection of the cubic gamma phase of Al_2O_3. The broadness of the peak is caused by the thin thickness of the oxide films. The relatively strong oscillation at small angle reflectivity on all of our oxide films grown on Si (111) indicates that the film thickness is highly uniform and smooth.

The single crystalline nature of the γ-Al_2O_3 film is further studied by scans along the major zone axes in reciprocal lattice. We find that γ-Al_2O_3 (004) peak lies on the same zone axis with the Si (004) reflection, proving that the film is single crystalline and is aligned with the Si (111)

The relatively strong oscillation at small angle reflectivity on all of our oxide films grown on Si (111) indicates that the film thickness is highly uniform and smooth. Note that the intensity measurement covers eight orders of magnitude, and shows our improved sensitivity to small signals. From the decay of intensity and the periodic oscillation of the collected signal (at small angle region), the oxide thickness and surface roughness were calculated to be about 3.8 nm and 0.13 nm. The surface morphology of the oxide films was routinely studied by AFM. From the observation of AFM measurement on the film 3.8 nm thick, the

root mean square (RMS) surface roughness was 0.126 nm, in agreement with the measured value using x-ray reflectivity.

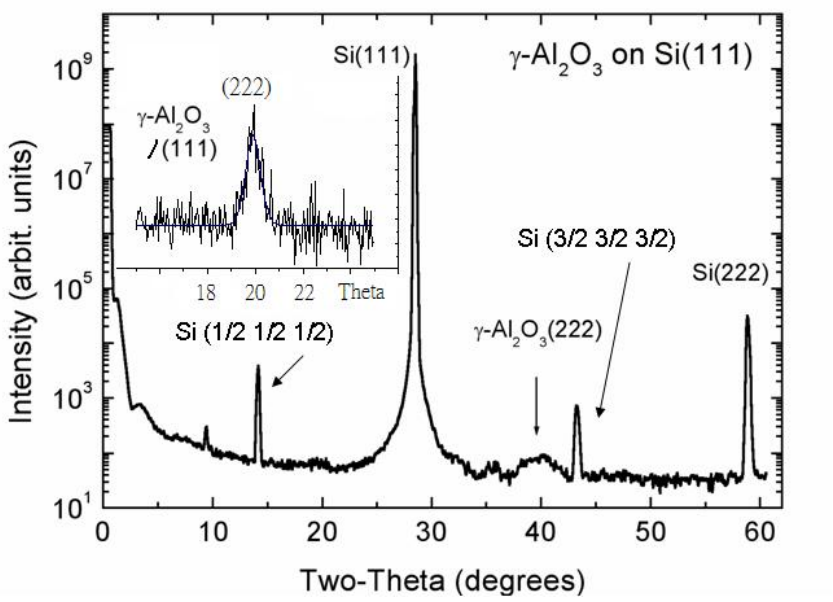

Fig. I-2 X-ray theta two-theta scan along Si (111) surface of (111) γ-Al_2O_3 film 3.8 nm thick and the mosaic scan of the γ-Al_2O_3 (222) peak.

The sample for TEM observations was prepared in two different thinning processes including wet and dry polishing (with and without water) prior to the ion milling. In general, for high-k gate dielectrics deposited on Si, during the thinning, water may be absorbed by the oxide dielectrics, diffuse through the interface and form silicon oxide or silicates. The cross-section TEM on our single crystal hetero-structure of γ-Al_2O_3/Si, nevertheless, shows that no silicon oxide was found at the interface, irrespective of wet or dry polishing. The results strongly indicate that our single crystal γ-Al_2O_3 films were water-resisted. The water-resisted characteristics provide advantageous properties to the usage of our single crystal γ-Al_2O_3 in the high-k gate dielectric applications.

The interface was found to be atomically sharp and smooth, as shown in Fig. 3(a) of HR-TEM, whose micrograph was taken with the electron beam directing along $[112]_{Si}$. In the inset of Fig. I-3 (a), the orientation relation in cross-sectional direction (Si [112]) was found to be Si (112) // Al_2O_3 (224), Si [$\bar{1}$ $\bar{1}$1] // Al_2O_3 [$\bar{2}$ $\bar{2}$2]. Electron diffraction

patterns from the plan-view of the hetero-structure (Fig. I-3 (b)) show Si (111) // Al_2O_3 (222), Si [220] // Al_2O_3 [440].

(a)

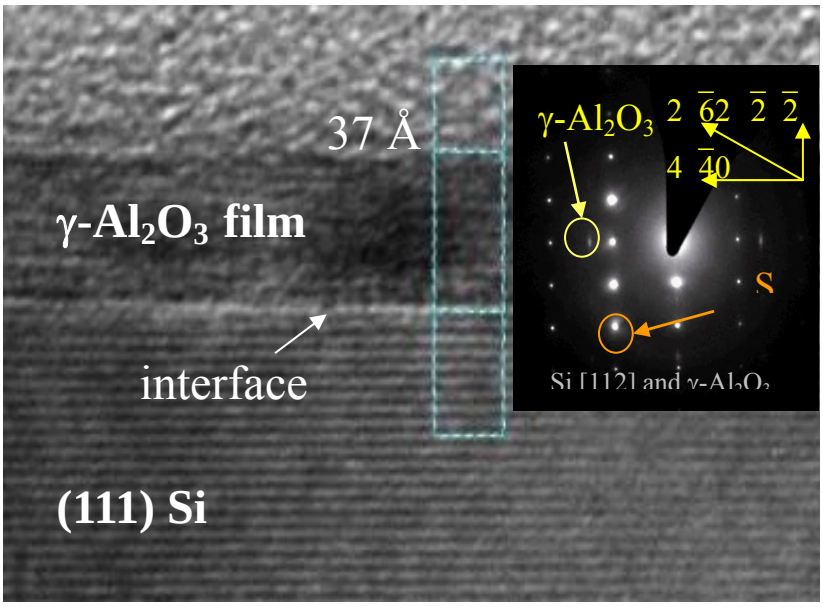

(b)

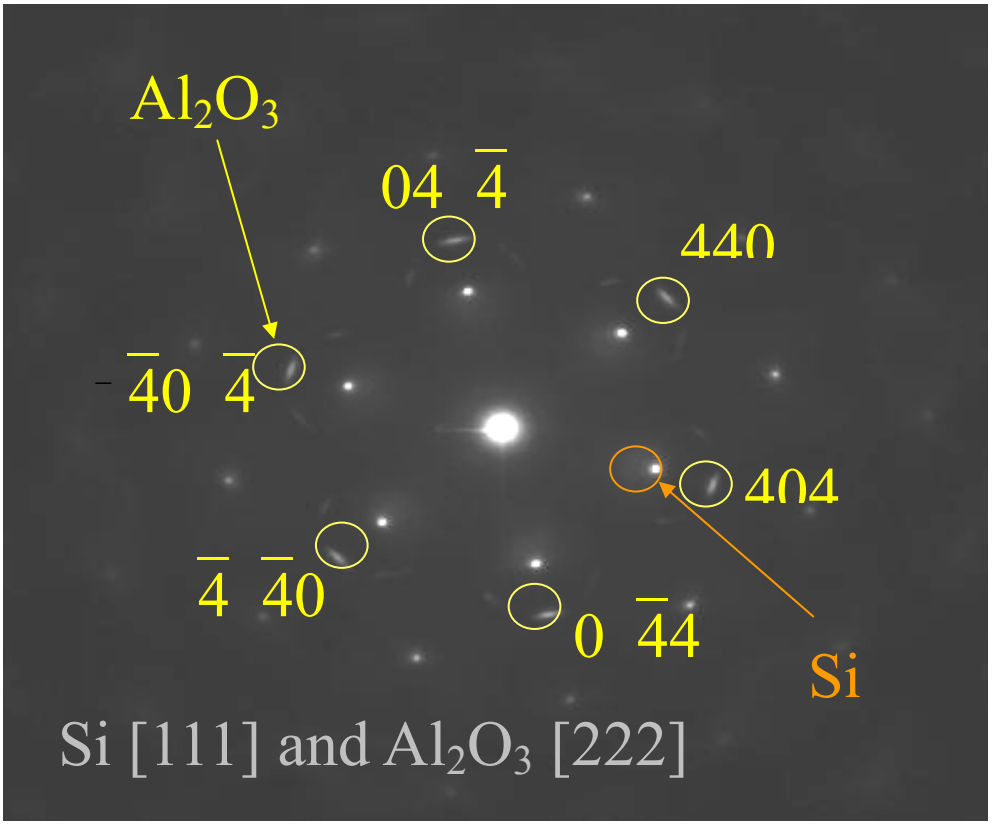

Fig. 3 Cross-sectional TEM image and electron diffraction pattern of a 3.8 nm γ-Al_2O_3 film, showing a sharp interface and smooth surface (a). The electron diffraction pattern indicates that the film is well aligned with Si substrate. The In-plane electron diffraction pattern of the 3.8 nm γ-Al_2O_3 film is shown in (b).

The distance of (440) plane of γ-Al_2O_3 from electron diffraction pattern (Fig. I-3 (b)) is 1.3936 Å, which is calculated from the distance ratio of the diffraction spots of Si substrate and γ-Al_2O_3 film along the direction of [440]. The distance of (440) plane obtained from the γ-Al_2O_3 films 3.8 and 11 nm thick is 1.3912 and 1.401 Å, respectively. The results are consistent with the XRD data base of 1.3984 Å.

The faint side-peaks observed in Fig. I-3(b) may be caused by multiple-diffraction, commonly observed in TEM. The faint spot on the right of Al_2O_3 (440) peak results from adding reciprocal lattice points Al_2O_3 (404) and Si (02 $\bar{2}$), while the faint spot on the left results from adding reciprocal lattice points Al_2O_3 (04$\bar{4}$) and Si (202). Similarly, all the side-peaks can be indexed by the multiple-diffraction of electrons in this system. The tangential broadening of the film peaks is consistent with the $\pm 3^0$ splitting of the x-ray peaks observed in the pole figure about Si (111). This broadening could be due to slight in-plane misalignment of the film with respect to substrate, in order to accommodate the lattice mismatch.

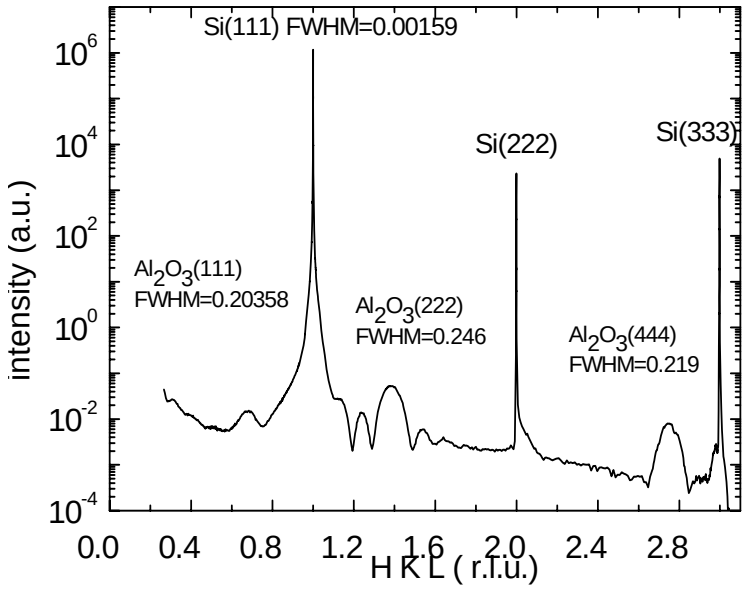

Fig. I-4 X-ray theta two-theta scan using synchrotron radiation on the same film shown in Fig. I-1

I (a)-4 Conclusion

The cubic γ-Al_2O_3 and Si have significantly different atomic structures and lattice constants. The lattice constant of γ-Al_2O_3 is 7.91Å and that of Si is 5.42 Å. Matching the two lattices over a unit cell dimension will result in a >30% lattice mismatch. It is intriguing that a highly ordered epitaxial growth was obtained in an unusually large mismatch for a hetero-epitaxial system.

Note that a more recent study using synchrotron radiation source at NSRRC has given much more detailed information on the crystallographic structures of both the thin film and the interface. This then will allow us to study γ-Al_2O_3 films with thickness in the range of 2 nm. ***In fact, an x-ray diffraction normal scan with synchrotron radiation on the same sample of Fig.I-1 is shown in Fig. I-4. In Fig. 1, the (222) peak of γ-Al_2O_3 has been barely revealed with a small broad peak. In a very strong contrast, all the peaks of γ-Al_2O_3 are now well resolved with sharp peaks using synchrotron radiation. The Pendellösung fringe oscillations surrounding the (222) are clearly exhibited, indicating a highly uniform film with an atomically smooth surface and sharp oxide/Si interface.***

(b) Sc_2O_3[9]

Brief Summary

High-quality single-crystal Sc_2O_3 films a few nanometer thick have been grown epitaxially on Si (111) despite a huge lattice mismatch. The films were electron beam evaporated from a Sc_2O_3 target. Structural and morphological studies were carried out by x-ray diffraction and reflectivity, atomic force microscopy (AFM), high-resolution transmission electron microscopy (HRTEM), and medium energy ion scattering (MEIS), with the initial epitaxial growth monitored by in-situ reflection high energy electron diffraction (RHEED). The films have the cubic bixbyite phase with a remarkably uniform thickness and high structural perfection. The film surfaces are very smooth and the oxide/Si interfaces

are atomically sharp with a low average roughness of 0.06 nm. The films are well aligned with the Si substrate with an orientation relationship of Si (111) // Sc_2O_3 (111), and an in-plane expitaxy of Si [$\bar{1}$10] // Sc_2O_3 [$\bar{1}$01].

I(b)-1 Introduction and Background

Sc_2O_3 has recently gained attention due to its effective passivation on GaN, and its usage as a gate dielectric in GaN based MOS devices[10]. Unexpectedly, Sc_2O_3 thin films were found to grow epitaxially on Si (111)[11,12] and sapphire[13] with excellent crystal quality. Sc_2O_3 is also attractive as an alternative gate dielectric for Si[12] due to its relatively high dielectric constant, large bandgap, and thermodynamic stability with Si. High-resolution x-ray diffraction studies on single crystal films 18 nm in thickness, e-beam evaporated from compacted powder pacts of Sc_2O_3 in ultra high vacuum (UHV), have shown a high-intensity and persistent Pendellösung fringe oscillations around the Sc_2O_3 (222) diffraction peak and narrow rocking curves of Sc_2O_3 (222) and (444)[11]. These films were of the bulk bixbyite cubic phase with high structural perfection, sharp interface with Si, and the (111) axis of the oxide films parallel to the substrate normal. The cone scans of the Sc_2O_3 {440} and Si {220} diffraction peaks about the surface normal indicated a 60^o symmetric rotation of the film with respect to the substrate. High-resolution transmission electron microscopy (HRTEM) studies by Klenov et al[12] on extended defects in a 35-nm thick epitaxial Sc_2O_3 film, prepared using reactive molecular beam epitaxy (MBE) with a Sc flux in an O_2 background, have shown the formation of a hexagonal misfit dislocation network and a high density of planar defects and threading dislocations.

In this Section, we report the attainment of very high-quality cubic Sc_2O_3 single crystal films with a thickness in the regime of 3 to 4 nm, at least six to ten times thinner than what were published earlier. These nano-scale films enable us to study the structural quality in the initial stages of growth, and to understand their interfacial characteristics, based on studies

using high-resolution x-ray diffraction in a synchrotron radiation source, x-ray reflectivity, HRTEM, and medium energy ion scattering (MEIS) (a lower energy, high resolution variant of Rutherford backscattering spectroscopy[14]).

I (b)-2 Experimental

HRTEM specimens were prepared with mechanical polishing, dimpling, and ion milling using a Gatan PIPS system operated at 3kV. HRTEM was performed on a field-emission microscopy (Tecnai G^2) operated at 200 kV.

Small-angle x-ray reflectivity provides valuable information about the film thickness, the interfacial roughness, and the electron density distribution[15]. By using the modeling fits of $Bede_{REFS}$ Mercury Code[16], we were able to determine these parameters. The synchrotron x-ray experiments were performed at wiggler beamline BL17B1 at the National Synchrotron Radiation Research Center (NSRRC), Hsinchu, Taiwan. The incident x-rays were focused vertically with a mirror and monochromatisized to 10keV energy by a Si (111) double-crystal monochromator. The sagital bending of the second crystal focused the x-rays in the horizontal direction. The dimensions of beam size are about 2 mm x 0.2 mm (H x V) at the sample position. With two pairs of slits between sample and detector, typical wave-vector resolution in the vertical scattering plane was set at ~ $0.01nm^{-1}$. High-resolution single-crystal x-ray measurements were carried out in the single crystal geometry.

Substrate Si (111) wafers were placed into a multi-chamber MBE/UHV system[8], following RCA-cleaning and HF dipping. A Si (111) surface with a streaky (7x7) RHEED pattern and Kikuchi lines were obtained following a wafer heating to ~750°C. The wafers were then transferred under UHV to an oxide chamber for the Sc_2O_3 deposition, in which electron beam evaporation of pure powder-packed Sc_2O_3 source at substrate temperatures in the range of 400-770°C. During the oxide deposition, the pressure in the chamber was in the low 10^{-9} torr range. After an ~0.7 nm thick oxide was grown, bright, streaky (4x4) RHEED

film patterns were observed along the major in-plane axes of Si ([$\bar{2}20$] and [$\bar{2}02$]), indicative of two-dimensional growth and an in-plane alignment between the oxide film and the Si substrate (not shown). After the oxide growth, a 2.4 nm thick amorphous Si cap layer was deposited in-situ on Sc_2O_3 for protection.

I (b)-3 Results and Discussion

The oxide films grow with their [111] axis parallel to the [111] Si substrate normal, and the [$\bar{4}04$] in-plane axis parallel with the substrate [$\bar{2}20$] direction. The rocking scans at Sc_2O_3(222) position of the 3 nm film show a small full-width-at-half-maximum (FWHM) of 0.03°, indicative of a high-quality single crystal oxide film. AFM showed a very smooth surface of a rms roughness of 0.1~0.2 nm. The oxide/Si interface is also atomically smooth with a value of 0.06 nm as determined by x-ray reflectivity, and is free of SiO_2 as found by cross-sectional HRTEM and MEIS.

Figure I-5 shows single-crystal scan in reciprocal space along the surface normal. The scattered intensity is displayed over nine-orders of magnitude of dynamic range, and the horizontal axis displacement is displayed in terms of reciprocal space units of the silicon substrate, i.e., the values of H, K and L given in this paper are expressed in reciprocal lattice units (r. l. u.) referred to the Si lattice parameter, 0.54309 nm at 295 K. For surface normal scan, reciprocal lattice unit vectors H, K and L are set equal to each other, and are all incremented by equal amounts. The broad range covered in Fig. I-5 displays substrate peaks (111) and (222), and also (222) and (444) peaks of the bixbyite phase of the Sc_2O_3 epitaxial film. Peak positions of the film along the surface normal agree well with the bulk lattice constant of Sc_2O_3, indicating that the epitaxial film is fully relaxed. The well defined fringe patterns about the Bragg peaks of the film confirm a highly uniform film thickness. The period of the fringe pattern suggests a film thickness of 3.4 nm, in agreement with a value of 3.59 nm determined from x-ray reflectivity (as shown in the inset of Fig. I-5)

The rocking scans of the substrate and the films observed in Fig. 1 show that the substrate Si(111) peak exhibits a FWHM value of 0.005°, while the film Sc_2O_3 peaks (222) and (444) exhibit FWHM values of 0.033° and 0.044°, respectively. The film peak shapes are not symmetric about the center, as would have been expected from fully strain relaxed film growth. Since relaxation incorporates structural defects like misfit dislocations at the interface (discussed later in the text), the film peaks will broaden in these rocking scans. Considering that the film is fully relaxed, these mosaic spread values are remarkably small. Other samples we measured correlated well with the reported sample. In these fully relaxed films rocking curve variations are not significant. Characteristic inclined defects can also explain the selective broadening of the (222) peak. Distinct crystallographic defects, like anti-phase boundaries, do selectively affect some of the Bragg peaks.

Figure I-6 shows a representative cross-sectional HRTEM image of the Sc_2O_3/Si(111) heterostructure along $[1\bar{1}2]_{Si}$ projection. A careful examination of the experimental contrast indicates the epitaxial growth of Sc_2O_3 on Si with the orientation relationship of $(111)_{Sc2O3}[1\bar{1}0]_{Sc2O3}$ // $(111)_{Si}$ $[1\bar{1}0]_{Si}$. Considering the symmetry elements of Sc_2O_3 (*Ia-3*), the electron diffraction based HRTEM, viewing in projection, cannot distinguish the in-plane rotation of Sc_2O_3 by 60°. Nevertheless, an edge-type misfit dislocation with the line direction parallel to $[1\bar{1}2]_{Si}$ can be observed (see "**T**" in Fig. I-6). Note that the same type of dislocation was recently reported in 35-nm-thick Sc_2O_3(111) films grown on Si(111) exhibiting a regularly spaced (~1.8 ± 0.1 nm) network,[12] in good agreement with the theoretical spacing of ~1.9 nm for a dislocation accommodated mismatch system. Compared to the work on relatively thick films,[12] the absence of a regular dislocation network in Fig. 6 could be a consequence of the film thickness. In ultrathin film heterostructures[17], the *elastic* accommodation of an in-plane misfit strain is believed to be a complementary strain relief mechanism to the dislocation network formation. Moreover, the kinetics of the elastic

accommodation can be complicated by the dynamic film growth conditions and the early nucleation characteristics[17], potentially leading to the absence of a dislocation network in our ultrathin films. However, the residual strain in the ultrathin Sc_2O_3/Si(111) may be further relaxed by the inclined defects in Sc_2O_3 (see the arrow in Fig. I-6). The particularly bright contrast at the interface (see Fig. I-6) could be also relevant to the strain effect, and a detailed study is under way.

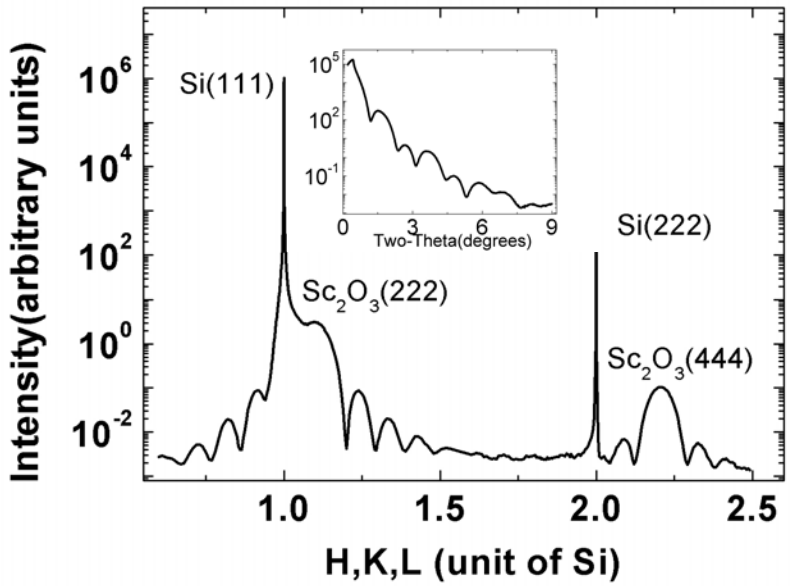

Fig. I-5 Single crystal scans along the surface normal in reciprocal space finds an epitaxial growth of the Sc_2O_3 bixbyite phase.

The density of the inclined defects in our sample was estimated to be ~10^{14} m^{-2}. This value is considerably low compared to that of the line defect, misfit dislocations (>10^{16} m^{-2}), frequently observed in epitaxial hetero-structures. Since neither considerable inclined defects nor extensive dislocation networks were observed in the current system, it is expected that the corresponding rocking scans are little affected by such crystallographic defects.

Figure I-7 shows a MEIS backscattering energy spectrum for an uncapped Sc_2O_3 film exposed to air prior to analysis. The measurement was done in a double alignment geometry in the Si [$\bar{1}\,\bar{1}\,2$] scattering plane, with the incoming beam aligned with a [111] channeling direction and the detector axis aligned with a Si [001] axis. Observation of distinct blocking

minima in Sc signal, shown in the inset in Fig. I-7, and comparison of the Sc signal just below the surface Sc peak to a calculated yield for the same thickness amorphous film (the yield, shown as a dashed line in Fig. I-7) indicates very good film crystalline quality.

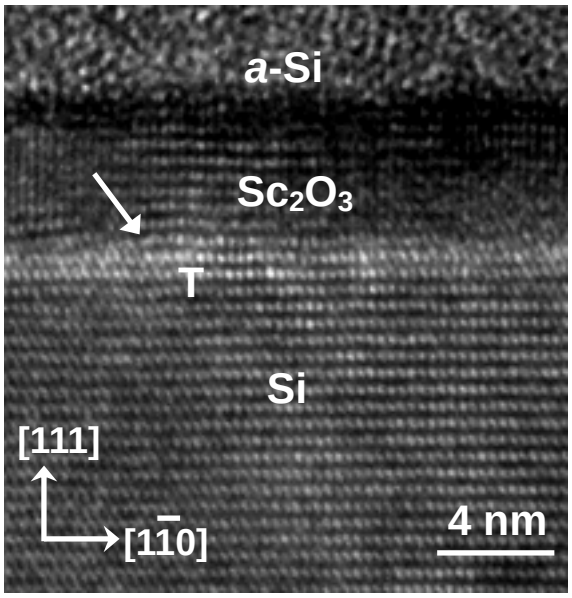

Fig. I-6 A cross-sectional HRTEM image of the Sc_2O_3/Si(111) heterostructure in $[11\bar{2}]_{Si}$ projection, showing the Sc_2O_3 film thickness of ~4 nm. The edge-type misfit dislocation is indicated by "**T**". The arrow exhibits the inclined defects in Sc_2O_3.

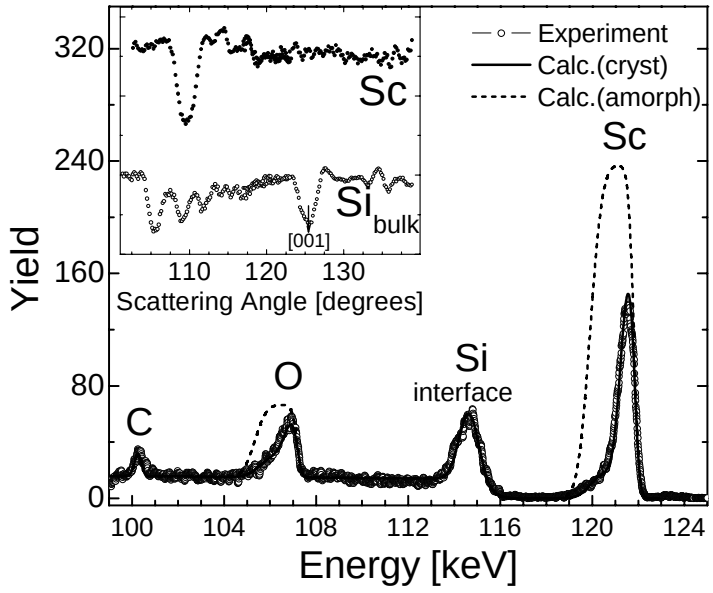

Fig. I-7 Backscattering energy spectrum (130 keV H^+) of a Sc_2O_3 film on Si(111) in a normal incidence and substrate blocking geometry. A simulation (solid line) shows a fit for a 3.9 nm thick crystalline film with no detectable interfacial layer formation, to be compared to a simulation for an amorphous film (dashed line). The inset shows angular distributions for the Si and Sc signals.

Surface carbon species were detected (~2×10^{15}atoms/cm^2) due to the air exposure.

Remarkably no interfacial Sc and O peaks are observed, indicating a highly ordered Sc_2O_3 lattice structure at the interface with Si. The small additional visibility of Si atoms at the interface (compared to an ideal, bulk terminated lattice) suggests good crystallinity of the interface with possibly some quite minor deformation or defect formation of the Si lattice.

I (b)-4 Conclusion

The films have the cubic bixbyite phase with a remarkably uniform thickness and high structural perfection. The film surfaces are very smooth and the oxide/Si interfaces are atomically sharp with a low average roughness of 0.06 nm. The films are well aligned with the Si substrate with an orientation relationship of Si (111) // Sc_2O_3 (111), and an in-plane expitaxy of Si $[\bar{1}10]$ // Sc_2O_3 $[\bar{1}01]$.

Sc_2O_3 and Si have significantly different crystal structures, different bonding, and lattice constants. The bulk lattice constants of Si (5.43 Å) and Sc_2O_3 (9.86 Å) are mismatched by 9.2 % (relative to the doubled Si unit cell dimension). It is intriguing that a highly ordered epitaxial growth was obtained with this unusually large mismatch.

References for Section I

1. S. Nakamura, et al, Appl. Phys. Lett. **64,** 1687 (1994)
2. R. A. Mckee, et al, M. F. Chrisholm, Phys. Rev. Lett. **81**, 3014 (1998).
3. J. Kwo, et al, Appl. Phys. Lett. **77**, 130 (2000).
4. S. Guha, et al, J. Appl. Phys. **90,** 512 (2001)
5. A. Wakahara, et al, J. Crystal Growth **236,** 21-25 (2002).
6. Young-Chul Jung, et al, Journal of Crystal Growth **196,** 88-96 (1999).
7. J. T. Zborowski, et al, J. Vac. Sci. Technol. **B 16(3)**, 1451 (1998).
8. M. Hong, et al, J. Vac. Sci. Technol. **B 14(3)**, 2297 (1996).
9. M. Hong, et al, Appl. Phys. Lett. **87**, 251902, 2005.

10. J. Kim, et al, Appl. Phys. Let. **81**, 1687, (2002).

11. C. P. Chen, et al, J. Crystal Growth **278**, 638 (2005).

12. D. O. Klenov, et al, Appl. Phys. Lett. **86**, 051901 (2005) and references therein.

13. A. R. Kortan, et al, Mat. Res. Soc. Symp. Proc. **811**, p. E1.2, (2004).

14. J. F. van der Veen, Surf. Sci. Rep. **5**, 199 (1985).

15. L. G. Parratt, Phys. Rev. **95** 359 (1954).

16. D. K. Bowen and B. K. Tanner, Nanotechnology, **4** 175 (1993).

17. M.-W. Chu, et al, Nature Mater. **3**, 87 (2004);

II. Growth and structural characteristics of GaN on nano thick γ-Al_2O_3 /Si (111) and Sc_2O_3/Si (111)

(a) GaN/*γ-Al_2O_3/Si (111)*

Brief Summary

We report on the growth of GaN by nitrogen plasma-assisted molecular beam epitaxy on 2" Si (111) substrates with a thin (~5.5 nm) single-crystal layer of γ-Al_2O_3 [1] as the buffer layer. Cubic γ-Al_2O_3 has a defective Spinel structure which is different from the more common corundum structure of α-Al_2O_3 (sapphire). Transmission electron microscopy and x-ray diffraction measurements indicated that the γ-Al_2O_3 was a single crystal, as was discussed in Section I(a) on a γ-Al_2O_3 (3.7nm thick)/Si(111). Reflection high-energy electron diffraction (RHEED) measurements (Fig. II-1) indicated an orientation relationship of GaN(0002)//γ-Al_2O_3(111)//Si(111) and GaN[1-100]//γ-Al_2O_3[4-2-2]//Si[4-2-2]. The orientation relationship has also been confirmed using x-ray diffraction and TEM. The cubic γ-phase of Al_2O_3 was first deposited on Si(111) substrate by electron-beam evaporation of a high-purity sapphire source. From RHEED observations, the initial stage of GaN growth showed a mixture of cubic and hexagonal domains. Further growth of GaN resulted in a streaky and bright RHEED pattern. No cracking was observed in the GaN layer with thickness around 1 μm when inspected with an optical microscope. More extensive structural characteristics on GaN/γ-Al_2O_3/Si (111) were studied using high-resolution x-ray diffraction and high-resolution transmission electron microscopy.

II(a)-1 Introduction

III-nitride compound semiconductors are suitable for applications in high-temperature and high-power electronics because of their wide band gaps, high breakdown fields and high saturation velocity in high fields. The epitaxial growth of GaN on silicon offers several advantages over that on sapphire or SiC, including substrates with high crystal-quality, cost advantages, and integration of high-power electronics and/or optoelectronics with the most

advanced integrated circuits (ICs). Directly growth of GaN on Si is extremely difficult, due to the large lattice mismatch of ~17% and difference in thermal expansion coefficients of ~33% between GaN and Si. Numerous intermediate layers, including AlN,[1,2] HfN,[3] SiN[4], and Al_2O_3 [5], have been employed to effectively facilitate excellent epitaxial growth of GaN on Si. Recently, nano-thick cubic γ-Al_2O_3 single crystal films epitaxially grown on Si (111) with high crystal quality have been obtained using electron beam evaporation under ultra high vacuum (UHV)[6], as was discussed in Section I (a). The in-plane symmetry of the gamma-Al_2O_3 films is similar to that of sapphire (0001) (alpha-Al_2O_3), which has been commonly used for GaN growth.

In this work, we have succeeded in achieving epitaxial growth of GaN using molecular beam epitaxy (MBE) on the γ-Al_2O_3/Si (111). In-situ reflection high energy electron diffraction (RHEED) has exhibited the initial growth of GaN (AlN), showing streaky patterns with a bright intensity, indicating an epitaxial growth right at the beginning. The epitaxial interfacial characteristics among GaN (AlN)/γ-Al_2O_3 and γ-Al_2O_3/Si, and the crystal defects including dislocations in GaN and γ-Al_2O_3 films have also studied using high-resolution transmission electron microscopy (HR-TEM). The interfacial chemical information has also been performed using x-ray photoelectron spectroscopy (XPS). The hetero-structures of GaN/γ-Al_2O_3/Si(111) has also been studied using high-resolution x-ray diffraction using synchrotron radiation source.

II(a)-2 Experimental

The detailed experimental procedure in achieving high-quality nano-thick single crystal γ-Al_2O_3 films on Si (111) was described in Section I (a). The samples of γ-Al_2O_3/Si were then transferred ex-situ to another MBE system for the GaN epilayer growth. The sample was out-gassed in the preparation chamber before loading to the growth chamber. The substrates

were exposed to nitrogen plasma to nitridate the surface. Group III elements (Ga, Al) and Si (n-type dopant) were evaporated using standard effusion cells. The details of the GaN growth were published previously.[7] After growth, the GaN had a streaky (2x2) RHEED pattern. The samples were then removed from the GaN MBE chamber and ex situ (exposed to air) transferred to the MBE system (mentioned in the first step) for deposition of the oxide films. The experimental details on HR-TEM (and the TEM sample preparation), HR x-ray diffraction, x-ray reflectivity, and in-situ RHEED are referred to Section I (a) and (b)-2 experimental.

II(a)-3 Results and Discussion

GaN films were directly nucleated on the thin γ-Al_2O_3 templates with/without an AlN buffer layer. The in-situ RHEED streak spacing of γ-Al_2O_3 is larger than that of GaN. Therefore the in-plane lattice constants in this direction are $a_{GaN} > a_{Al2O3}$. The benefit of our work is that the growth of nitrides on γ-Al_2O_3 coated Si (111) has put the nitride films in a compressive strain, which helps prevent cracking from occurring. If nitrides are grown directly on Si(111), GaN tends to crack after a certain thickness due to tensile strain.

However, the adsorption of Ga is very weak on γ-Al_2O_3 at high temperatures. Only the substrate temperature was reduced to about 580-600^oC significant adsorption of Ga on the surface can be observed based on the dimming of the RHEED pattern. Therefore, we started the nucleation at about 580-600^oC. Relaxation occurs almost immediately (which is expected due to the large lattice mismatch) and the evidence of co-existence of mixed cubic and wurtzite domains was revealed from the RHEED pattern (similar to low temperature GaN buffer layers on sapphire). When high temperature growth is commenced, the RHEED pattern becomes very streaky after a few minutes.

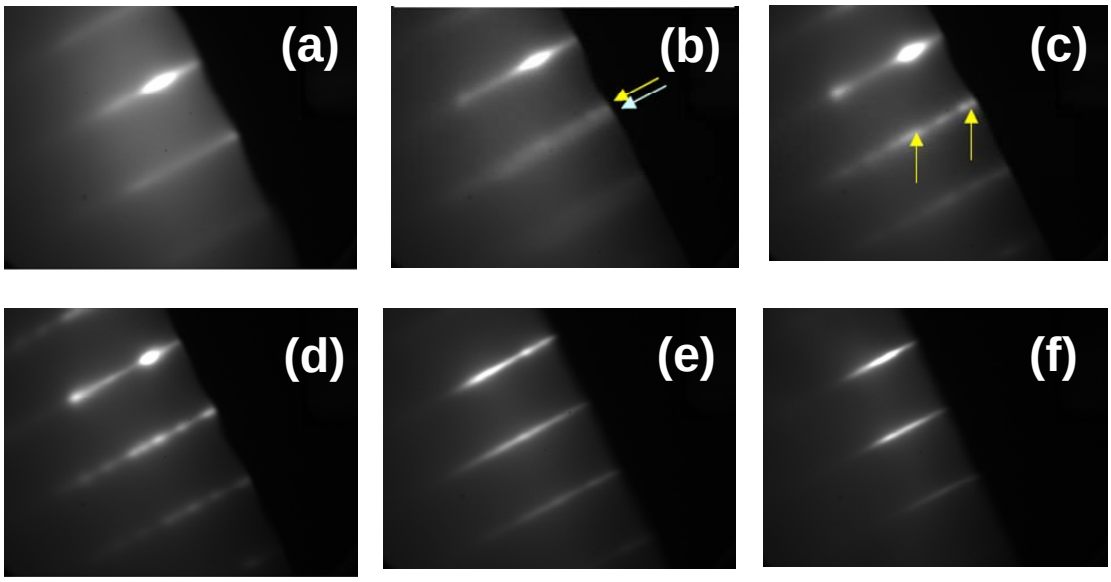

Fig. II-1 Real-time Reflection High-Energy Electron Diffraction of different stages (a) γ-Al_2O_3 at low temperature(~200°C) (b) 10 sec. of GaN growth (~580°C), (notice the formation of GaN streaks in addition to theγ-Al_2O_3RHEED streaks, indicating relaxation) (c) 20 sec. of GaN growth (~600°C), (notice the cubic spots appearing) (d) (e) (f) are the 1min., 5min., and 50min.GaN growth (~720°C), respectively. The "streakiness" of the GaN pattern improves as a function of time.

Fig. II-2 shows the data of high resolution x-ray diffraction of the sample of GaN/γ-Al_2O_3/Si(111). From the peak position and peak intensity, the wurzite GaN (0002) and γ-Al_2O_3 (222) peaks can be defined clearly. The FWHM of the theta rocking scan is 0.4482° (see the inset figure) which is carried out at GaN (0002) peak position. This means the GaN film grown on top of γ-Al_2O_3 buffer has good quality. Moreover, the thickness of GaN film grown on γ-Al_2O_3 is about 0.2 μm. This thickness is too thin to a well develop GaN structure. Thus the FWHM of theta rocking will be smaller if the thicker GaN film is grown. From the phi-cone scan, the symmetry and alignment of the films and substrate can be figured out. From the normal-plane theta-two theta scan the GaN(0002)//γ-Al_2O_3(111)//Si(111) can be determined. The in-plane orientation were determined to be GaN[1-100]//γ-Al_2O_3[4-2-2]//Si[4-2-2] from the phi-cone scan of the out-off-plane Bragg peaks. Furthermore, the coherent length of GaN along the growth direction, estimated from the (00*l*) line width analysis using the Williamson–Hall plot, is about 190 nm. This indicates the structural coherence of the GaN layer maintains over almost the entire layer thickness.

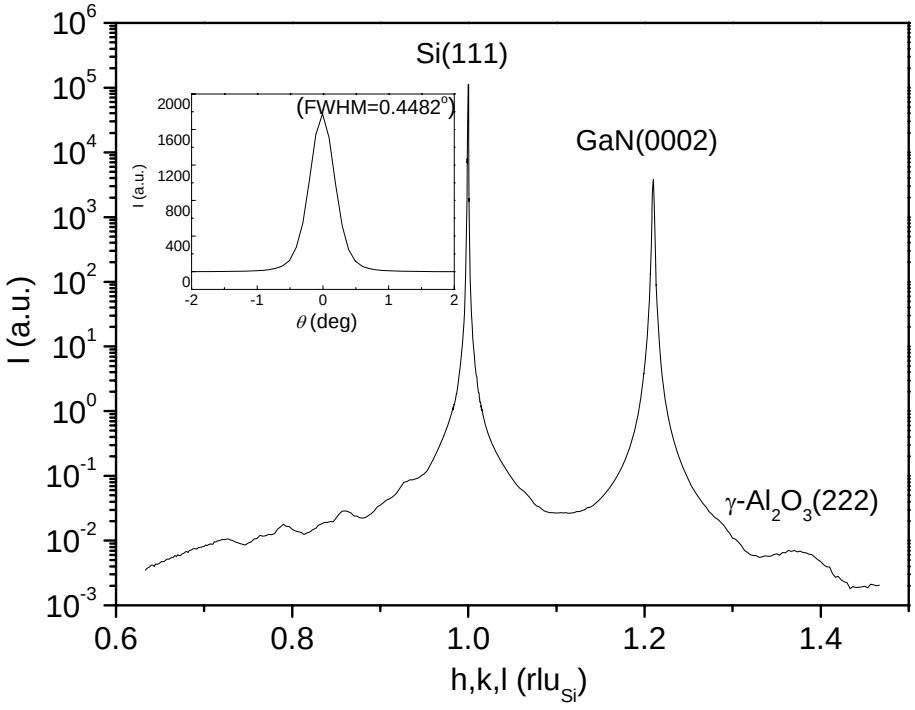

Fig. II-2 Radial scan along surface normal of a GaN/γ-Al_2O_3/Si(111) sample. The th-rocking curve of GaN (0002) reflection is illustrated in inset.

Better-quality GaN may be achieved on our improved γ-Al_2O_3 films, comparing with those previous grown GaN on Al_2O_3 films of less quality.[2,3] Experimental efforts have been planned to grow GaN on the γ-Al_2O_3 films discussed and achieved in Section I(a).

TEM studies on the hetero-structure of GaN/γ-Al_2O_3/Si (111) were performed with a cross-sectional micrograph shown in Fig. II-3. The GaN layer thickness is 0.3 μm. Both γ-Al_2O_3 and its interface with Si have remained intact as observed from TEM, even they have been subjected to very severe conditions, such as growth temperatures of ~750°C and nitrogen plasma bombardments.

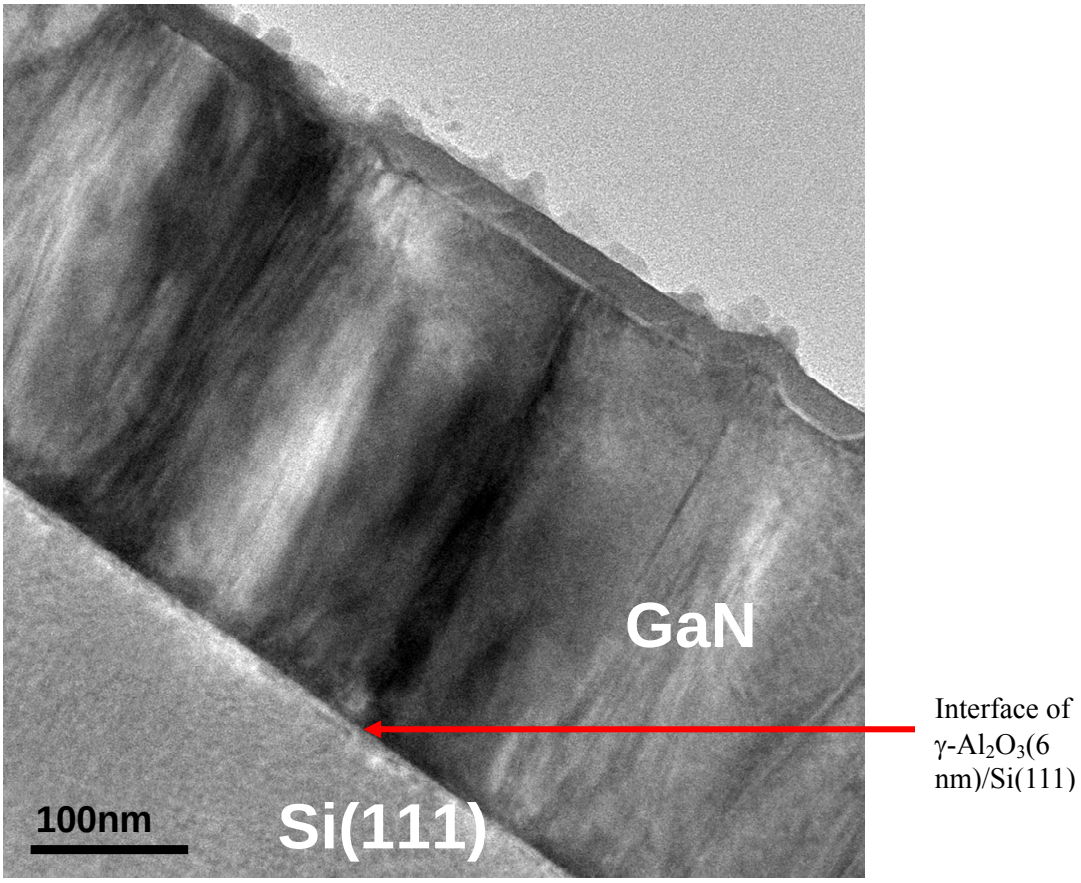

Fig. II-3 A cross-sectional micrograph of GaN/γ-Al_2O_3(6 nm)/Si(111) hetero-structure. Note that there is no low-temperature grown AlN as an intermediate layer.

(b) GaN/*Sc_2O_3/Si (111)*

Brief summary

We report on the growth of GaN by plasma-assisted molecular beam epitaxy on Si(111) substrates with a thin (~19.3 nm) single-crystal layer of Sc_2O_3 as a template layer. We have systematically studied the structural properties of the samples by using high-resolution transmission electron microscopy (HR-TEM), high-resolution x-ray diffraction (HR-XRD) using synchrotron radiation, and in-situ reflection high energy electron diffraction (RHEED). X-ray diffraction measurements indicated an orientation relationship of GaN(002)//Sc_2O_3(111)//Si(111) and Si[22-4]//GaN[100], with Sc_2O_3[22-4] rotating by 60° with respective to Si[22-4], i.e. B-type orientation. The growth of GaN resulted in a streaky

and bright RHEED pattern. No cracking was observed in the GaN layer with thickness around 0.2 μm when inspected with an optical microscope.

II (b)-1 Introduction

III-nitride compound semiconductors are suitable for applications in high-temperature, high-power electronics because of their wide band gaps, high breakdown fields and high saturation velocity in high fields. Due to a large gate leakage of the III-nitride based metal-semiconductor field-effect transistors (MESFETs) and high electron mobility transistors (HEMTs) resulting from the Schottky barrier gate, there has been a great interest in the development of III-nitride-based metal-oxide-semiconductor field-effect-transistors (MOSFETs) because of their relatively low leakage currents, power consumption and capability of greater voltage swings. GaN is typically grown on sapphire substrates, which is not cost-effective. In this work, we have used nano thick single crystal Sc_2O_3 epitaxially grown on Si (111) as templates for growing GaN. Single crystal Sc_2O_3 thin films, which are thermodynamically stable with Si and have been grown epitaxially on Si(111)[6], are used as the buffer (template) layers. Sc_2O_3 films were bixbyite cubic phase with high structural perfection, sharp interface with Si, and the (111) axis of the oxide films parallel to the Si substrate normal. The subsequent single-crystalline growth of GaN on the insulating layers (which were deposited on Si) may realize the integration of high-power microwave devices or lasers with the most advanced Si-based electronic devices

II(b)-2 Experimental

E-beam evaporation was used to evaporate the high melting point of high-purity Sc_2O_3 oxide source in MBE/UHV system. During the oxide deposition, the vacuum in the chamber was maintained in the $6x10^{-8}$ torr, even with the oxide evaporation, and the Si (111) substrate temperature was kept at ~800°C. Streaky RHEED patterns were observed after growth of oxide, indicating the attainment of a smooth single crystal oxide film formed on Si (111), as

was discussed in Section I(b).

The samples of Sc_2O_3/Si were then transferred ex-situ to another MBE system for the GaN epilayers growth. The sample was out-gassed in the preparation chamber before loading to the growth chamber. The substrates were exposed to nitrogen plasma to nitridate the surface. Group III elements (Ga, Al) and Si (n-type dopant) were evaporated using standard effusion cells. After growth, the GaN had a streaky (2x2) RHEED pattern. The samples were then removed from the GaN MBE chamber and ex situ (exposed to air) transferred to the MBE system (mentioned in the first step) for deposition of the oxide films.

Figure 1 shows a sequence of real-time RHEED images taken at different stages of the growth. Fig. 1(a) reveals a (4x4) reconstruction for the high quality Sc_2O_3 film grown on Si(111)[6]. The sample was out-gassed in the preparation chamber without any other cleaning after being transferred ex-situ from the other MBE system, in which the oxide was deposited. Followed by AlN and GaN epilayers growth, as shown from the RHEED images, a sequence of line scans was taken from the RHEED images, cross sections of the streak pattern taken perpendicular to the streaks, indicated that the AlN relaxes almost immediately due to the large lattice mismatch. When GaN is first deposited on the AlN, it is first strained and then relaxes as the thickness increases. Also the full width at half maximum (FWHM) of the streaks is decreasing as the growth proceeds. Therefore, the "streakiness" of the GaN pattern improves as a function of time. At the end of the GaN growth, a (2x2) reconstruction RHEED pattern was observed, indicating a Ga polarity surface. On the other hand, judging from the RHEED streak spacing, with the largest for AlN, followed by GaN and Sc_2O_3, the in-plane lattice constants are $a_{Sc2O3} > a_{GaN} > a_{AlN}$.

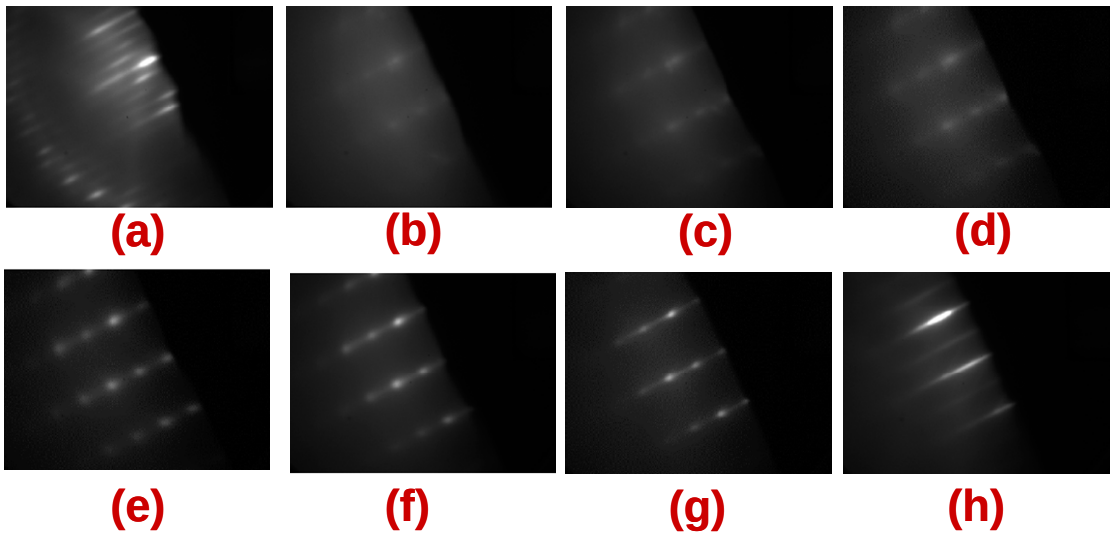

Fig. II-4 Real-time Reflection High-Energy Electron Diffraction of different stages (a) Sc_2O_3 at low temperature(~200°C) (b) 10 sec. of GaN growth (~580°C), (notice the formation of GaN streaks in addition to the Sc_2O_3RHEED streaks, indicating relaxation) (c) 20 sec. of GaN growth (~600°C), (notice the cubic spots appearing) (d) (e) (f) are the 1min., 5min., and 50min.GaN growth (~720°C), respectively. The "streakiness" of the GaN pattern improves as a function of time.

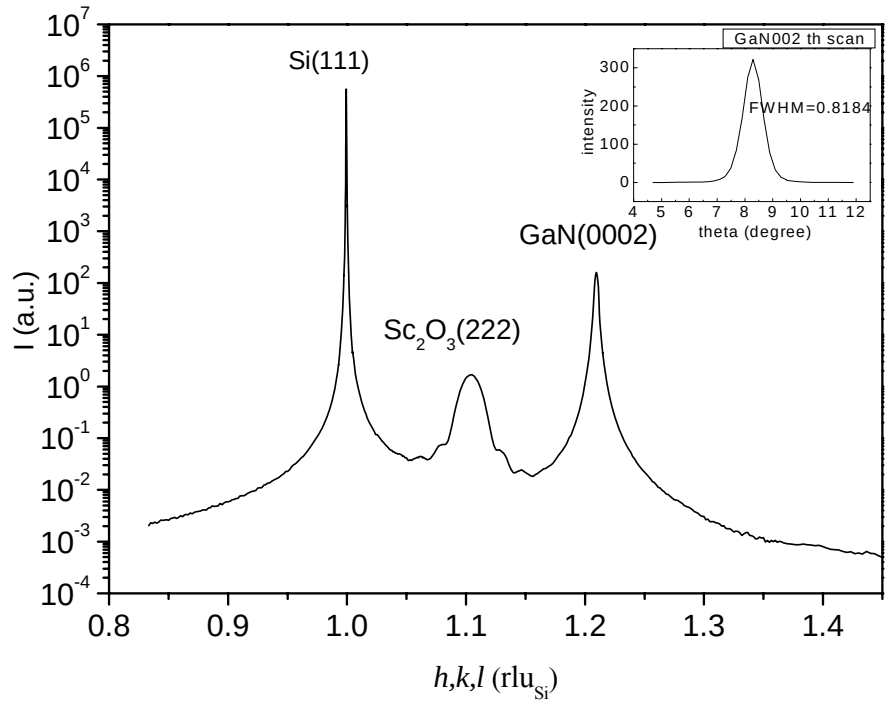

Fig. II-5 (a) Radial scan along surface normal. The observation of Si (111), Sc_2O_3 (222) and GaN (0002) reflections manifests the GaN (0002) surface is aligned with the Si (111) and Sc_2O_3 (111) surface normal. Inset shows the th-rocking curve at the GaN (0002) reflection which yields a mosaic spread of 0.8°.

Figure II-5 shows the structural analysis by X-ray diffraction, which was were performed at wiggler beamline BL17B1 at the National Synchrotron Radiation Research Center, Hsinchu, Taiwan. X-ray L scan along surface normal across (a) Si (003), and (b)Si (006) reflections are

shown below which indicate the Sc_2O_3 films are well aligned with Si substrate with an orientation relationship of Si(111)//Sc_2O_3(111)//GaN(0002). The inset in Fig. II-5(a) shows the th-rocking scan at the GaN (0002) peak position, exhibiting a FWHM of 0.82°.Furthermore, the locations of off-specular reflections reveal the in-plane epitaxial relationship of GaN[1-100]//$Sc_2O_3[22\bar{4}]$//Si$[4\bar{2}\bar{2}]$. This is an evidence of the film is indeed a single crystal.

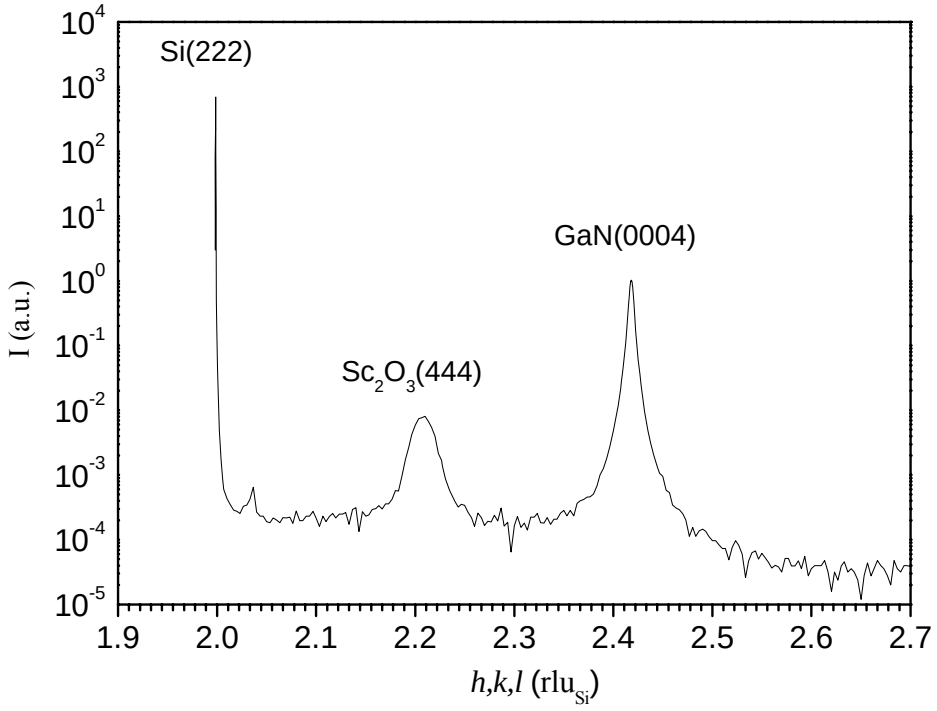

Fig. II-5 (b) Radial scan along surface normal across Si(222) reflection.

Figure II-6 show a typical cross-sectional high resolution TEM image of the GaN/Sc_2O_3/Si (111) hetero-epitaxial structure, the GaN epi-layer was grown by plasma-assisted molecular beam epitaxy. The inset in the right corner shows the Sc_2O_3 between the Si and GaN epi-layers. Due to our unique MBE approach, the interface exhibits an abrupt transition from semiconductor to oxide. The high quality Sc_2O_3 films serve as a template for the GaN growth, the film thickness of GaN, and Sc_2O_3 is 0.2μm, and 19.3nm, respectively. Due to the lattice mismatch between GaN/Sc_2O_3 the dislocation is shown in the

image. The density of dislocations shown in Fig. II-6 may be less than that of GaN grown on sapphire as shown in Fig. III-1. However, a detailed comparison needs to be conducted with a more systematic study on the characteristics, such as Burger vectors, of the dislocations in these GaN epilayers. There seems to be some interactions between GaN and Sc_2O_3 during the GaN growth, whereas the interactions between GaN andγ-Al_2O_3 seem less.

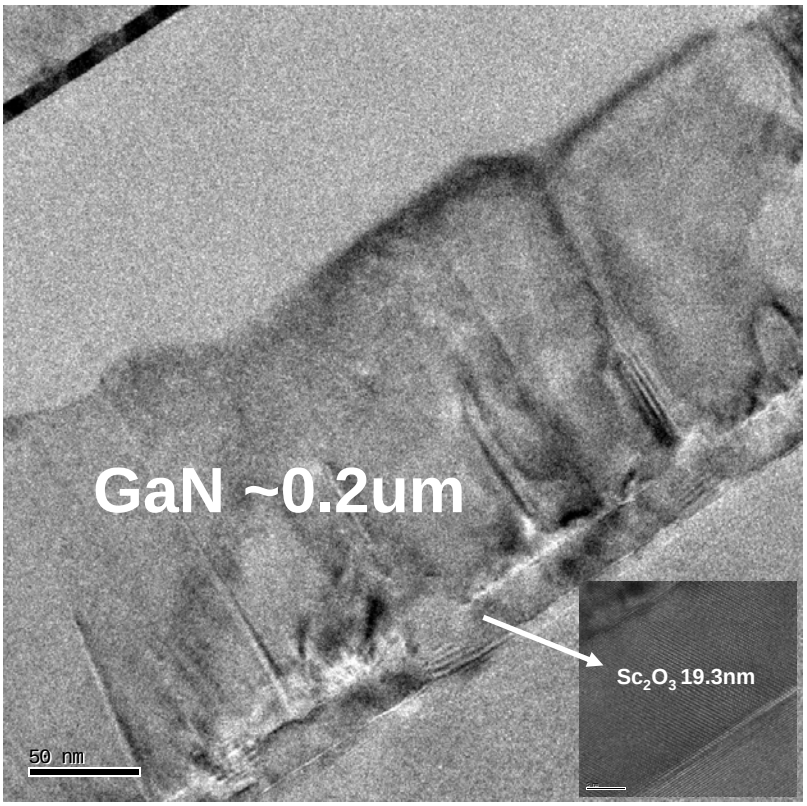

Fig. II-6 Cross-sectional TEM of GaN/Sc_2O_3/Si (111) with a magnified view of Sc_2O_3/Si (111) and the interface shown in the inset.

III. Growth of GaN on c-plane sapphire Al_2O_3 using MOCVD and/or MBE

Most commonly, high-quality GaN has been grown on c-plane sapphire using MOCVD and/or MBE. The growth procedure has been published extensively with a necessity of employing an intermediate layer AlN (or GaN) grown at low temperatures with bulk of III-nitrides grown at high temperatures, namely above 750°C for GaN using MBE and above 900°C using MOCVD. Here, we have studied the structural characteristics of both MBE-GaN and MOCVD-GaN using TEM and x-ray diffraction, respectively.

Figure III-1 has shown a cross-sectional transmission electron microscopy study on a hetero-structure of GaN/Gd_2O_3(1.8nm thick)/GaN(0.64μm thick)/α-Al_2O_3 (sapphire). Take a note on the interface between the first GaN and sapphire substrate, namely the low temperature grown intermediate or nucleation layer, ~0.1 μm thick and the GaN immediately above it. There is a high density of dislocations and the defect network, which is to be compared with the dislocations and defects exhibited in Figs. II(a)-3 and II(b)-3. The characteristics of the dislocations and defects of GaN (or AlN) grown on α-Al_2O_3 (sapphire) and those on γ-Al_2O_3 and cubic Sc_2O_3 seem to be different, however, they need to be studied in more detail. For comparison, the characteristics of the dislocations and defects in GaN grown on α-Al_2O_3 (sapphire) are apparently different from those on thin single crystal Gd_2O_3, as shown in Fig. III-1.

XTEM of GaN/Gd_2O_3(24Å)/GaN(0.64 μm)/Al_2O_3

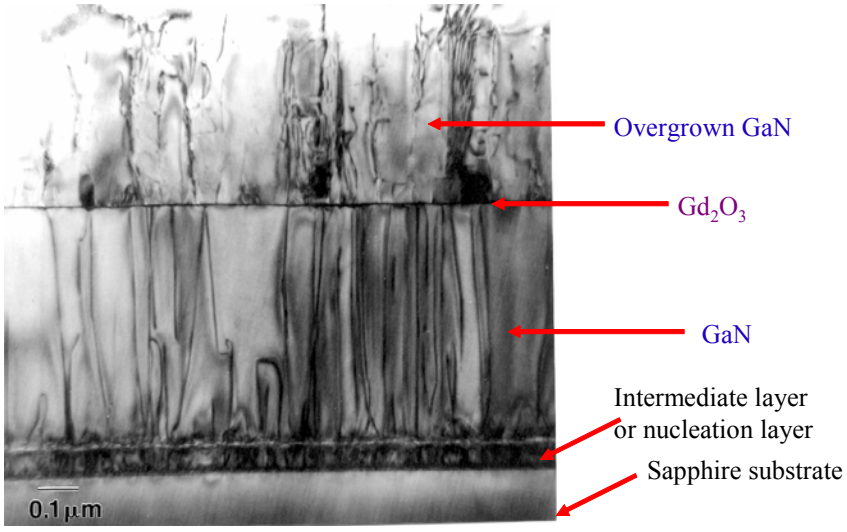

Fig. III-1 cross-sectional TEM micrograph of hetero-structure of GaN/Gd_2O_3(1.8nm thick)/GaN(0.64μm thick)/α-Al_2O_3 (sapphire).

High resolution x-diffraction using synchrotron radiation has been used to study structural characteristics of GaN ~2μm thick. Figure II-2 shows a theta-two theta scan on such an epi layer grown on sapphire substrate. The FWHM of the GaN (0002) peak is very narrow of 0.00426°, a value comparable to 0.00421° of the substrate sapphire (0002) approaching the resolution limit of the instrument. Moreover, the rocking scan on the GaN peak gave a small FWHM of 0.084°, again indicating, indeed, the excellent crystallinity of the GaN ~2μm thick. In comparison, a FWHM of 0.0063° has been obtained in a GaN epilayer ~0.3 m thick deposited on γ-Al_2O_3, with a rocking curve of 0.4482°, which is five times higher than that of the thinner GaN. A much meaningful comparison will be conducted on GaN epilayers with thickness over 2μm grown on sapphire substrates as well as on nano-thick γ-Al_2O_3 and cubic Sc_2O_3 epitaxially grown on Si (111). The GaN growth conditions may be adjusted for achieving optimized nitride films for different substrates.

Illustrated in Fig. III-2 is the radial scan along surface of a sample of Y_2O_3 doped HfO_2 (YDH)/GaN/sapphire. The presence of GaN (0002) and (0004) reflections together with the (0006) reflection of sapphire reveals the good alignment of the basal planes of GaN and sapphire. In addition, the broad peak centered at 1.75 rlu_{GaN} originates from the (111) plane of cubic-phase YDH layer, which is also aligned with the GaN basal plane. The narrow line width of GaN(0002) th-rocking curve 0.08°, as shown in the inset, indicates the very high crystalline quality of the GaN film In addition, the pronounced thickness fringes around YDH (111) Bragg peak evidences the sharpness of the YDH/GaN interface.

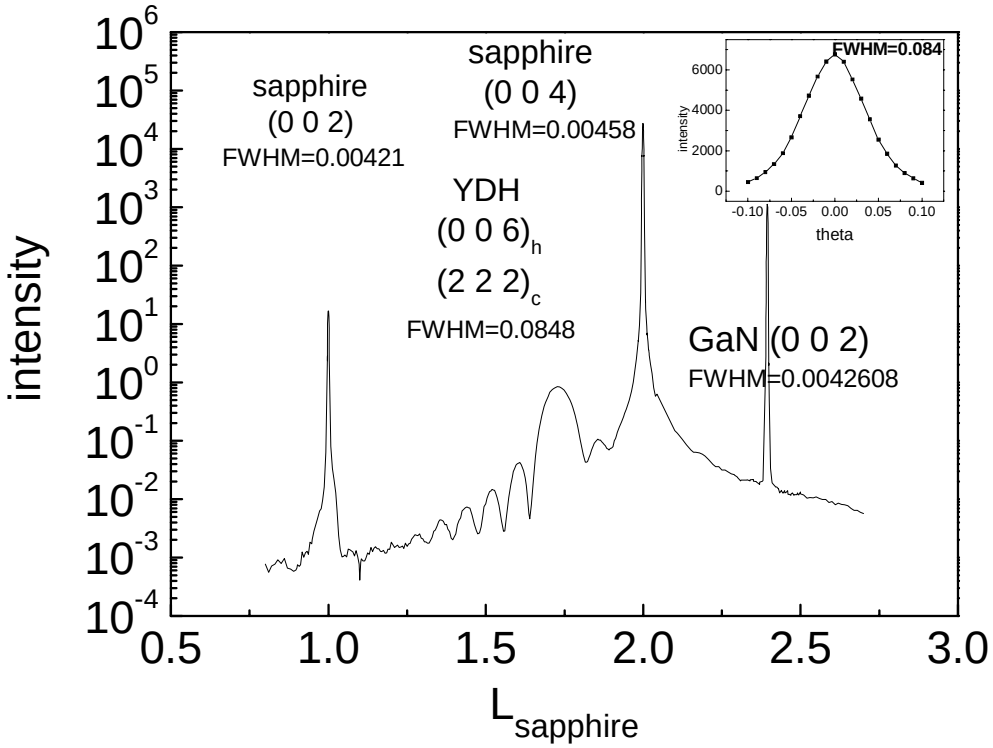

Fig. III-2

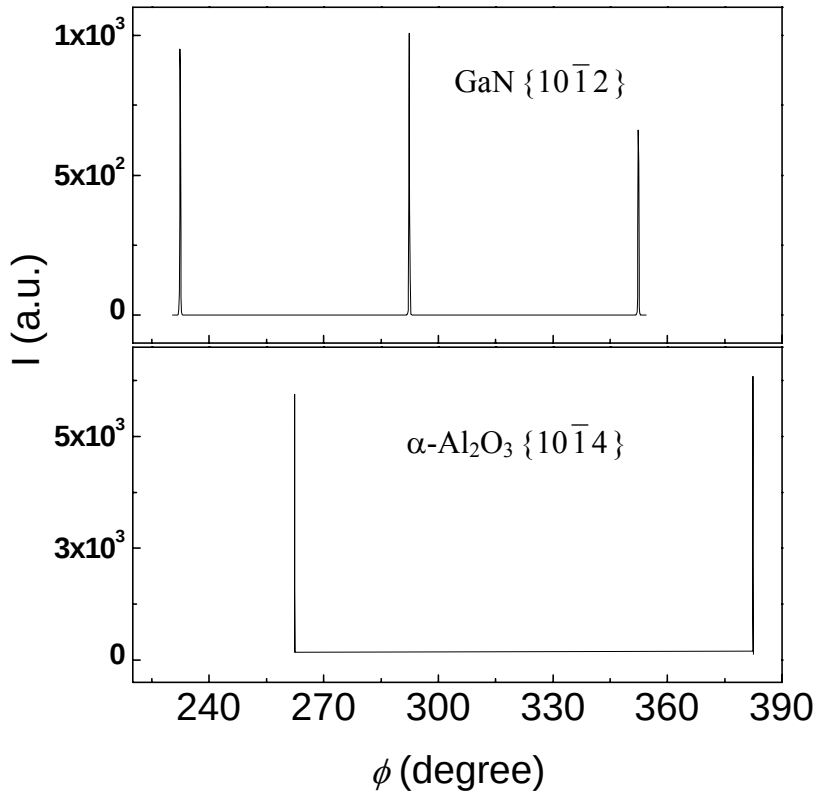

Fig. III-3 Azimuthal scans across off-specular (top panel) GaN $\{10\bar{1}2\}$ and (bottom panel) α-Al_2O_3 $\{10\bar{1}4\}$ reflections.

Figure III-3 illustrates the ϕ-cone scans across sapphire $\{10\bar{1}4\}$ and GaN $\{10\bar{1}2\}$, respectively. The former shows the characteristic 3-fold symmetry of rhombohedral structure along body diagonal and the later exhibits 6-fold symmetry, characteristics of wurtzite structure. Obviously, the $(10\bar{1}0)$ reflections of GaN and sapphire are rotated 30° against each other.

We have demonstrated that epitaxial GaN layers are grown on substrates of c-plane sapphire or Si (111) wafers with γ-Al_2O_3 or Sc_2O_3 buffer layers. FWHM's of GaN (0002) th-rocking curve and $(10\bar{1}1)$ ϕ–scan are summarized in table I. Even though the of line widths of GaN grown on c-plane sapphire is smaller, the crystalline quality of the GaN grown on Si(111) with buffer layers are very impressively good.

Table I. Line width of th-scan across specular (0001) and ϕ-scan across off-normal $(10\bar{1}1)$ reflections of GaN layers grown on various substrates/buffer layers.

GaN/Sapphire (0001)		GaN/Sc_2O_3/Si(111)		GaN/γ-Al_2O_3/Si(111)	
(0002)	FWHM(θ)=0.08°	(0002)	FWHM(θ)=0.82°	(0002)	FWHM(θ)=0.45°
$(10\bar{1}1)$	FWHM(ϕ)=0.2°	$(10\bar{1}1)$	FWHM(ϕ)=0.95°	$(10\bar{1}1)$	FWHM(ϕ)=1.62°

References

1. S. Nakamura, T. Mukai, and M. Senoh, Appl. Phys. Lett. **64**, 1687 (1994)
2. S. Guha, et al, J. Appl. Phys. **90,** 512 (2001)
3. A. Wakahara, et al, J. Crystal Growth **236,** 21-25 (2002).
4. S. Y. Wu et al, Appl. Phys. Lett. 87, 091908, (2005).
5. M. Hong, et al, Mater. Res. Soc. Symp. Proc. **811**, D9.5, Ed. by J. Morais, M. Houssa, D. Landheer, R.M. Wallace, published by Materials Research Society, Warrendale, PA.
6. M. Hong et al, unpublished results.
7. C. P. Chen, Journal of Crystal Growth 278, 638 – 642, (2005).

IV Technical Milestones for 2007:

1. ***optimization of GaN growth using MBE and MOCVD on single crystal γ-Al_2O_3 and other oxides epitaxial grown on Si (111)***
2. ***structural studies on hetero-structures of GaN/nano-thick γ-Al_2O_3 (and other oxides)/Si (111) using high-resolution x-ray diffraction using synchrotron radiation***
3. ***structural studies on hetero-structures of GaN/nano-thick γ-Al_2O_3 (and other oxides)/Si (111) using high-resolution transmission electron microscopy***

We have delivered what was agreed on the milestones of 2006.